Physical Characterization of Acoustic Communication Channel Properties in Underwater Mobile Sensor Networks

Andrea Caiti, Emanuele Crisostomi, and Andrea Munafò

ISME, Interuniversity Research Centre on Integrated Systems for the Marine Environment,
c/o DSEA, Dept. Electrical Systems and Automation, University of Pisa,
Largo Lucio Lazzarino (già via Diotisalvi 2), 56100 Pisa, Italy
{caiti,munafo}@dsea.unipi.it, emanuele.crisostomi@gmail.com

Abstract. A methodology to predict underwater acoustic channel communication properties (capacity, bandwidth, range) from the environmental conditions in the ocean is proposed. The methodology is based on the use of acoustic propagation models coupled to a set of equations proposed firstly by Stojanovic [1]. A parametric study of channel characteristics as a function of changing environmental conditions is presented, showing in particular how channel range and/or source transmission power are influenced by the relative position of source and receiver with respect to the ocean temperature thermocline. This kind of results is crucial to adaptively configure the relative position of mobile nodes (typically AUVs – Autonomous Underwater Vehicles) in underwater sensor networks, with the final goal of mitigating the effects of environmental changes on the network communication capabilities.

Keywords: AUV, underwater sensor networks, underwater communication, underwater acoustics, acoustic propagation.

1 Introduction

Since the seminal work of Curtin *et al.* [2], many progresses have been made toward the operational implementation of Autonomous Ocean Sampling Networks (AOSN). In particular, advances in miniaturization and embedded systems technology has now made possible the design and realization of low-cost Autonomous Underwater Vehicles (AUVs) [3], [4], that, equipped with appropriate oceanographic payloads, can act as a team in mapping specific areas of the ocean. Cooperation and coordination algorithms for mobile robotic vehicles have been successfully applied to teams of AUVs and/or oceanographic gliders [5]. Some large scale experimentation, in which networks of mobile and fixed sensors, autonomous or semi-autonomous, have been employed to monitor the evolution of ocean dynamics, have been successfully reported [6]. Nevertheless, the challenges posed by the ocean environments are such that there are still scientific and technological problems to be solved for the realization of the original AOSN vision.

S. Hailes, S. Sicari, and G. Roussos (Eds.): S-Cube 2009, LNICST 24, pp. 111–126, 2009.

One challenge not yet solved is related to the problem of communication among the underwater platforms, either fixed or mobile, composing the sensor network. Since electromagnetic waves are so strongly attenuated in salty waters to prevent any radio communication at distances exceeding few meters, acoustic waves are used for underwater communication. Hence, the physics of underwater acoustic propagation plays a key role in the determination of the communication channel characteristics. In turn, the physics of acoustic propagation is strongly influenced by the oceanographic conditions, since the sound speed in the water is a function of temperature, salinity and depth, and these quantities vary both in space and in time [7]. While several approaches have been proposed to model the underwater acoustic communication channel (see for instance [8] for a recent review), there still appears to be a gap in the scientific literature between the channel characterization which is required for communication system design, and the physical modeling of acoustic propagation.

In an attempt to bridge the above mentioned gap, Stojanovic [1] has proposed a set of expressions to determine maximum channel capacity and bandwidth as a function of the intensity loss of the acoustic signal. In [1], analytical computations are given for the case in which the medium (i.e., the ocean channel) is homogeneous and the intensity loss is due only to geometrical spreading and to the intrinsic attenuation of the medium. However, intensity loss is among the parameters computed by acoustic propagation codes: so, at least in principle, the approach of [1] can be extended in a straightforward manner by using appropriate numerical models of the acoustic channel.

The contributions of this paper are twofold:

- it is shown how indeed a specific computational code (the code "Bellhop", based on ray theory [7], [9]) can be used in order to derive communication channel characteristics following the approach of [1]; in doing this, we also discuss the set of modifications and/or caveat that have to be considered before transposing directly the results of the model into the channel equations.
- a parametric study based on the above mentioned channel modeling is performed to determine the variability of the communication channel performance as a function of the variability of the environmental conditions (and therefore of the acoustic propagation conditions).

The sensitivity study is directed toward the determination of optimal strategies for mobile nodes motion in an AOSN to maximize communication performance or to maintain team communication connectivity [10], [11]. While this latter problem is not treated in this paper, the results reported here are instrumental to the implementation of cooperative distributed motion algorithms in underwater sensor networks.

The paper is organized as follows: in the next section the main aspects of acoustic propagation relevant to the communication problem are briefly reviewed, the approach of [1] to the modeling of the acoustic communication channel reported, and the assumptions, validity limits and implementation choices adopted in coupling the physical model Bellhop to the communication channel equations illustrated. In Section 3 the simulative scenarios are described; in particular, we consider three cases, and in all of them sound speed changes only as a function of depth in the water column, but not of range between transmitter and receiver: in one case the sound speed is constant with depth (similar to the analytical case of [1]), in the other two cases a thermocline region is considered (i.e., a region in which temperature, and hence sound

speed, has a constant gradient with depth), and transmitter and receivers are located within the thermocline, or on opposite sides of the thermocline. Simulations for the three cases are referred to two different scenarios, one taken from the original Stojanovic paper [1], and the other, considering higher frequencies and shorter ranges, corresponding to a more realistic operational configuration. Conclusions and future work are addressed in Section 4.

2 Acoustic Propagation and Communication Channel Characterization

In this section we first review the physics of acoustic propagation and the assumptions of the ray modeling approximation. Subsequently, the channel characterization proposed in [1] is reported and linked to the ray model.

2.1 The Physics of Acoustic Propagation

The pressure field generated by an acoustic (compressional) wave traveling in the ocean medium is governed, in the linear approximation, by the Helmholtz equation [7]:

$$[\nabla^2 + k^2(\mathbf{x})]\psi(\mathbf{x},\omega) = f(\omega)\delta(\mathbf{x}-\mathbf{x}_s) \tag{1}$$

where ω is the angular frequency, $\mathbf{x}$ is the position in the space coordinate frame, ∇^2 is the Laplacian operator, $k(\mathbf{x}) = \omega / c(\mathbf{x})$ is the wavenumber, $c(\mathbf{x})$ is the sound speed in the medium as a function of geographical position, $f(\omega)$ is the forcing term due to a point source at location $\mathbf{x}_s$, δ is the Dirac's delta function, ψ is the wave potential. The pressure is related to the wave potential by the equation:

$$p(\mathbf{x},\omega) = \rho\omega^2\psi(\mathbf{x},\omega) \tag{2}$$

where ρ is the medium density, and it is considered constant in the following. To solve the Helmholtz equation it is necessary to specify the boundary conditions, in terms of sea surface and bottom depth, and the medium characteristics, in terms of the sound speed in the medium, which in practice depends on the ocean dynamics. The coordinate reference frame is usually taken with the origin at the sea surface and the z axis pointing downward toward the sea bottom. By assuming the existence of a solution to the homogenous Helmholtz equation of the form:

$$p(\mathbf{x},\omega) = e^{j\omega\tau(\mathbf{x})}\sum_{h=0}^{+\infty}\frac{a_h}{\omega^h} \ . \tag{3}$$

and substituting (3) into equations (1) and (2), neglecting the terms where ω appears at the denominator, one gets the *ray-theory approximation* equations:

$$\left|\nabla^2 \tau(\mathbf{x})\right| = \frac{1}{c^2(\mathbf{x})} \qquad \textit{(eikonal equation)} \qquad (4)$$

$$2\nabla\tau \cdot \nabla a_0 + (\nabla^2 \tau) a_0 = 0 \qquad \textit{(transport equation)} \qquad (5)$$

where $\tau(\mathbf{x})$ is the time of arrival of an acoustic ray from the origin to the position $\mathbf{x}$. The above derivation has been outlined to emphasize that the ray theory approach, which is followed since now on, due to its intuitive appeal, it is an approximation which is valid only in the high frequency regime (usually above the KHz).

In qualitative terms, using the ray approximation, an acoustic wave traveling from a source in the ocean water column will manifest itself as a sequence of arrivals corresponding to the various rays (Fig.1, left). Different rays will arrive at the receiver following different paths (multi-path arrivals). The paths themselves will be determined by the sound speed in the medium through the Snell's refraction law (which is embedded in the eikonal equation). In (Fig. 1, centre) a typical sound speed profile as a function of depth is shown. The corresponding ray paths are shown in (Fig. 1, right) assuming cylindrical coordinates and sound speed constant with range.

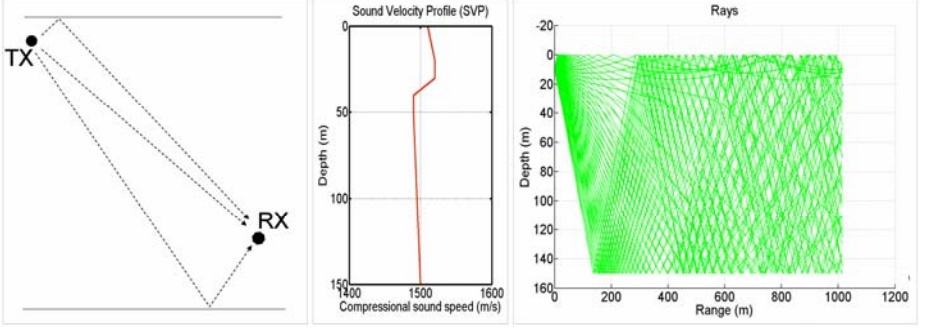

Fig. 1. The geometry of the transmitter and the receiver is shown on the left. Rays can arrive to the destination following different paths. A typical sound speed profile is shown in the middle, while the corresponding ray paths are shown on the right.

The acoustic intensity $I(\mathbf{x})$ is the power per unit surface of an acoustic wave, and it is proportional to the square of the pressure. The *transmission loss TL* of an acoustic wave is defined as:

$$TL(\mathbf{x}, \omega) = -10 Log_{10}\left(I(\mathbf{x}, \omega) / I_0\right). \qquad (6)$$

where I_0 is the reference intensity. In underwater acoustics, the reference intensity is the intensity of a plane wave having rms pressure amplitude of $1\mu Pa$ at 1m distance from the source. By numerical solution of the transport equation, it is possible to numerically compute *TL* in the ray approximation. The computational code "Bellhop"

[9] is such a code; it is widespread in the scientific community, having passed the appropriate recognized benchmark tests. In the following of the paper, all the simulative results will be obtained through Bellhop. Moreover, in all our simulations we will refer to the so-called "range independent" environmental conditions: a cylindrical coordinate frame will be assumed, with axis r (range) and z (depth); the source is always placed on the $z = 0$ axis, and $c(r, z) = c(z)$.

It is important to remark that the Bellhop model includes the following physical mechanisms of intensity loss: the geometrical spreading, computed along the paths for each ray; the intrinsic attenuation, which is the attenuation due to mechanical and thermodynamic effects of pressure propagation in salty water, and which is frequency dependent; the wave interference patterns due to the superposition of different rays.

The transmission loss can be used to predict the intensity level *S* at the receiver due to a source of intensity *SL* through the so-called *passive sonar equation*:

$$S(\mathbf{x}) = SL - TL(\mathbf{x}) \tag{7}$$

By considering also an ambient noise term, the passive sonar equation can be formulated in terms of the Signal-to-Noise Ratio (SNR) at the receiver as follows:

$$SNR(\mathbf{x}, \omega) = SL - TL(\mathbf{x}, \omega) - N(\omega) \tag{8}$$

where all the above quantities are in dB ref $1\mu Pa$ @1m. The same SNR can be expressed in natural scale as: $snr(\mathbf{x}, \omega) = I(\omega)/n(\omega)$. The ambient noise term $N(\omega)$, or $n(\omega)$ in natural scale, may depend on a series of factors (ship traffic, wave motions,…) and the noise model defined in [1], [12], is considered in the remainder of this paper, with the same parameter choices of [1]. Space limitations prevent to report the model here.

For any given source position $\mathbf{x_s}$, and for any receiver position $\mathbf{x}$ and any frequency ω it is possible to define the channel transfer function $G(\mathbf{x_s}, \mathbf{x}, \omega)$ satisfying the following relation between transmitted and received pressure:

$$p(\mathbf{x}, \omega) = G(\mathbf{x_s}, \mathbf{x}, \omega)\, p_s(\omega)\,. \tag{9}$$

where $p_s(\omega)$ is the source signal. The transmission loss can also be computed from the transfer function as:

$$TL = -20Log_{10}\left|G(\mathbf{x_s}, \mathbf{x}, \omega)\right|. \tag{10}$$

while the SNR in terms of transfer function is given as:

$$SNR = -10Log_{10}\left(snr\right) = -10Log_{10}\left(\frac{p_s^2\left|G\right|^2}{n}\right). \tag{11}$$

2.2 Acoustic Communication Channel Characterization

This section reports the definitions and equations proposed in [1] to characterize an acoustic communication channel on the basis of the transmission loss (equation (6)), of the SNR (equations (8) and (11)) and of the channel transfer function (equation 9). The original equations of [1] are slightly reformulated here to better link them to the physical description of the previous section, but preserving the same approach and considerations of [1]. We first note that, for any source-receiver geometric configuration $(\mathbf{x_s}, \mathbf{x})$ it is possible to define an optimal transmission frequency as:

$$\omega_0(\mathbf{x_s}, \mathbf{x}) = \arg\max_{\omega} \frac{\left|G(\mathbf{x_s}, \mathbf{x}, \omega)\right|^2}{n(\omega)}. \tag{12}$$

A *heuristic 3-dB bandwidth* $B_3(\omega_0)$ can then be defined as the range of frequencies in the neighborhood of ω_0 such that $SNR(\omega) > SNR(\omega_0) - 3$. For any given transmitted source signal $p_S(\omega)$, the source intensity in the bandwidth $B_3(\omega_0)$ is proportional to the square of the pressure spectrum integrated over the bandwidth:

$$I_S \propto \int_{B_3} p_s^2(\omega) d\omega. \tag{13}$$

The SNR, expressed in natural scale, within the 3dB bandwidth, is thus obtained by integrating the argument of the Log function in equation (11) over the bandwidth:

$$snr_{B_3}(\omega) = \frac{\int_{B_3} p_s^2(\omega)\left|G(\omega)\right|^2 d\omega}{\int_{B_3} n(\omega) d\omega}. \tag{14}$$

Equation (14) can then be used to dimension the source level (through $p_S(\omega)$) in order to achieve a prescribed SNR gain. In particular, assuming a constant source level p_3 over the 3dB bandwidth, in order to obtain a prescribed SNR γ (in natural scale) the following relation must hold:

$$p_3^2 \geq \gamma \frac{\int_{B_3} n(\omega) d\omega}{\int_{B_3} \left|G(\omega)\right|^2 d\omega}. \tag{15}$$

The corresponding channel capacity is given as:

$$C_3 = \int_{B_3} \log_2 \left(1 + \frac{p_3^2 \left|G(\omega)\right|^2}{n(\omega)}\right) d\omega. \tag{16}$$

As observed in [1], the above heuristic definition does not guarantee the optimality in the energy distribution across the system bandwidth. Therefore, in [1] it is proposed also the following approach, termed *capacity-based bandwidth definition*, in which the bandwidth is indeed defined in order to maximize the channel capacity. In particular, under the assumption of time-invariance of the channel, by subdividing the bandwidth in sub-bands of width $\Delta\omega$ such that the channel transfer function G can be considered constant within the sub-band and the noise term n white within the sub-band, the channel capacity for a receiver located in **x** is given by:

$$C(\mathbf{x}) = \sum_h \Delta\omega \log_2 \left(1 + \frac{p_s^2(\omega_h)\left|G(\omega_h)\right|^2}{n(\omega_h)} \right). \tag{17}$$

The optimal energy distribution within the bandwidth is obtained by maximizing the capacity in equation (17) with the constraint of finite transmitted power $\int p_s^2$. The optimal signal power spectrum must satisfy the water-filling principle [13]:

$$p_s^2(\omega) + \frac{n(\omega)}{\left|G(\omega)\right|^2} = \kappa. \tag{18}$$

where the constant κ is determined from the resulting signal power. The SNR corresponding to the optimal energy distribution is obtained as:

$$snr(\omega) = \frac{\int_B p_s^2(\omega)\left|G(\omega)\right|^2 d\omega}{\int_B n(\omega) d\omega} = \kappa \frac{\int_B \left|G(\omega)\right|^2 d\omega}{\int_B n(\omega) d\omega} - 1. \tag{19}$$

and the transmitted power is:

$$P_S = \int_B p_s^2(\omega) d\omega = \kappa B - \int_B \frac{n(\omega)}{\left|G(\omega)\right|^2} d\omega. \tag{20}$$

Once a prescribed SNR γ (in natural scale) is given, the following iterative procedure can be employed to determine the optimal energy distribution:

1. For each receiver position **x**, the optimal transmission frequency (equation 12) is determined; $\kappa(0)$ is initialized as $\kappa(0) = n(\omega_0)/2\left|G(\omega_0)\right|^2$ (note that κ will vary with receiver position)
2. given $\kappa(m)$, determine the bandwidth $B(m)$ as the region of frequencies around ω_0 such that $\kappa(m) > n(\omega_0)/\left|G(\omega_0)\right|^2$;
3. compute $snr(m)$ from equation (19) using $B(m)$ and $\kappa(m)$;
4. if $snr(m) < \gamma$, set $\kappa(m+1) = \kappa(m) + \varepsilon$, with ε (small) constant and go to step 2; otherwise, exit with $\kappa = \kappa(m)$ and $B = B(m)$

The optimal energy distribution is then given by equation (18) for $\omega \in B$, and it is zero outside the bandwidth B. The corresponding channel capacity, which will be referred as optimal channel capacity in the remainder of the paper, is given by:

$$C = \int_B \log_2 \kappa \frac{|G(\omega)|^2}{n(\omega)} d\omega . \tag{21}$$

2.3 Channel Performance from Acoustic Propagation Computation

The channel characteristics defined in the previous subsection can be determined by computation of the quantities defined in equations from (7) to (11) with a numerical code able to solve the Helmholtz equation (1). In particular, in the next section the code Bellhop, as already anticipated, will be extensively used. Bellhop solves equations (4) and (5), producing a high-frequency approximation of the solution of equation (1). One specific aspect has to be discussed when using the transmission loss computation from a numerical code as Bellhop to determine the communication channel performance: the evaluation of the multipath structure. In time domain the multipath structure reveals itself as a sequence of attenuated, delayed replicas of the first arrival, usually well separated in time (at least at high frequencies). Computational codes as Bellhop consider stationary sources and stationary waves; this implies, roughly speaking, that the signal intensity at the receiver position $\mathbf{x}_s$ is determined by adding up (with a coherent or incoherent procedure, depending if phase information is taken into account, and both options are available) the contributions carried on along each ray path to produce the total received intensity. As a result, in the case of coherent constructive interference, or in the incoherent case, multipath arrivals contribute to *decreasing* the transmission loss and *increasing* the SNR. While this makes sense in the usual application of acoustic propagation codes (determination of sonar ranges, etc.), it may not always be appropriate in the context of acoustic communication. An underwater acoustic communication signal will not transmit stationary waves, but it will use some kind of modulation. Multipath arrivals may not concur to enhance the SNR, but in fact, more often than not, will consist in a disturbance echo resulting in symbolic interference. Indeed, several receiving schemes proposed in the literature are based on the estimation of the multipath time-delay structure and on the suppression of the delayed arrivals [8].

It has to be noted, however, that there are propagation conditions in which only bottom reflected or surface reflected arrivals can reach the receiver; moreover, depending on the attenuation properties of the bottom (the "bottom loss"), a late surface reflected arrival may carry more power than a faster, bottom reflected arrival. In this case it is more useful to use the second arrival in decoding the transmitted signal.

Last but not least, it is worth to mention that other propagation codes, not based on the ray approximation, may cope with the same problem in a different way. For instance, when using normal mode-based computational codes, only the modes that effectively contribute to the useful part of the signal must be considered, while those contributing to symbolic interference must be discarded.

As a consequence of the above discussion, the decision whether to include the multipath arrivals in the computation of the transmission loss and of the SNR must ultimately depend on the modulation/demodulation algorithms and on anticipation of

some peculiarities in the propagation behaviour. In the simulations reported in the next section, we have *not* considered multipath arrivals; all else being equal, inclusions of the multipath structure would have led to an increase in the estimated performance of the channel. This means that the results obtained are valid only for those demodulating schemes that suppress the delayed echoes due to the multipath structure and for situations in which a direct path is always present between transmitter and receiver.

3 Simulations and Sensitivity Analysis to Sound Speed Variation in the Water Column

In this section we consider two different scenarios and three cases for each scenario. The first case is indicated as "nominal scenario", and it is similar to that analyzed in [1]: frequencies vary from 10 Hz to 20 KHz, transmitter-receiver ranges vary from 1Km to 100Km. The nominal scenario has been included in order to allow an easy comparison between our computational results and the analytical results reported in [1]. The second case is indicated as "operative scenario", since it is closer to the expected frequencies and ranges that are or may be used in AOSN applications: frequencies vary between 20 and 50 KHz, and transmitter-receiver ranges vary from 100m to 6000m. In both scenarios, three cases are considered with different environmental conditions: constant sound speed profile (equivalent to the analytical case of [1]); presence of a thermocline with both transmitter and receiver in the thermocline region; presence of a thermocline with the transmitter above the thermocline and the receiver below. The transmitter depth is 300 m above the receiver depth in the nominal scenario, and 100 m above the receiver depth in the operational scenario. The results are always reported as a function of the *horizontal* range between transmitter and receiver. Water depth and bottom absorption do not play any role since we are considering only direct arrivals. The sound speed profile varies with depth (hence the presence of a thermocline) but not with range (*range independent* environmental conditions).

In both scenarios, the following results have been produced and presented as graphical output for the three cases considered: SNR as a function of frequency; optimal frequency as a function of range; heuristic bandwidth and capacity; optimal bandwidth and capacity; source power required to reach a 20 dB gain in SNR as a function of range.

3.1 Nominal Scenario

The three cases considered for the nominal scenario, in terms of relative position and sound speed profile in the water column, are reported in Fig. 2. The gradient in the sound speed profile corresponds to the thermocline region. In the simulations, frequencies from 10Hz to 20KHz have been considered, with 100Hz spacing starting from 100Hz. Horizontal range varies between 1 and 100Km; 200 range slices have been considered.

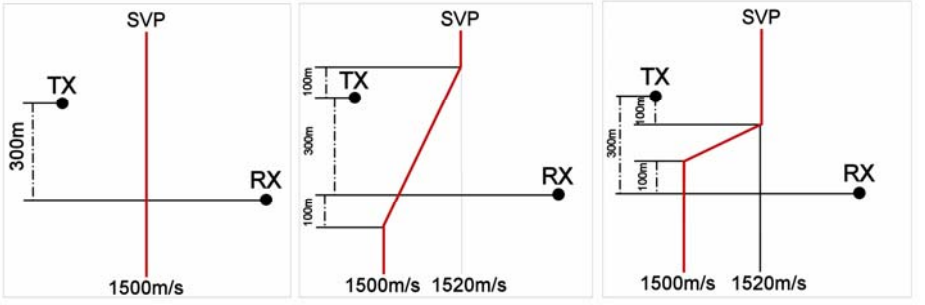

Fig. 2. The three cases considered, with different speed profiles as a function of depth, from the left to the right

In Fig. 3 the SNR as a function of range is reported for the three cases. The SNR decreases when propagation within the thermocline is considered. Note that in case 3, at 5 km distance, there is a direct path between the transmitter and the receiver that does not cross the thermocline.

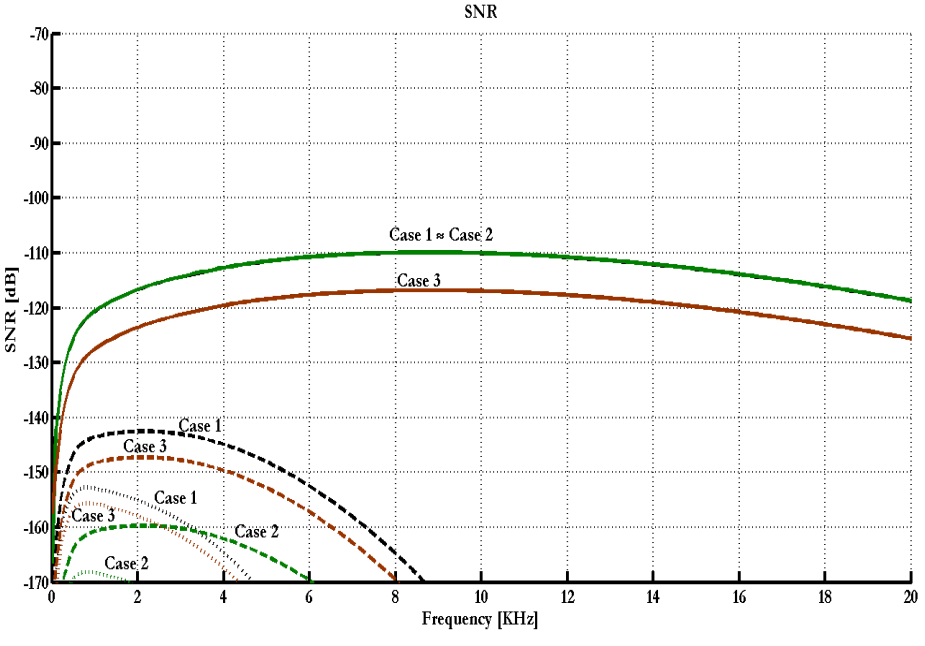

Fig. 3. SNR as a function of frequency. Solid lines refer to a range of 5 Km, dashed lines to range equal to 50 Km and dotted lines to 100 Km. For each of the three ranges, graphs corresponding to three cases are shown.

In Fig. 4 the optimal propagation frequency is indicated for the three cases; here it is worth to note that the optimal frequency is not influenced by the propagation condition.

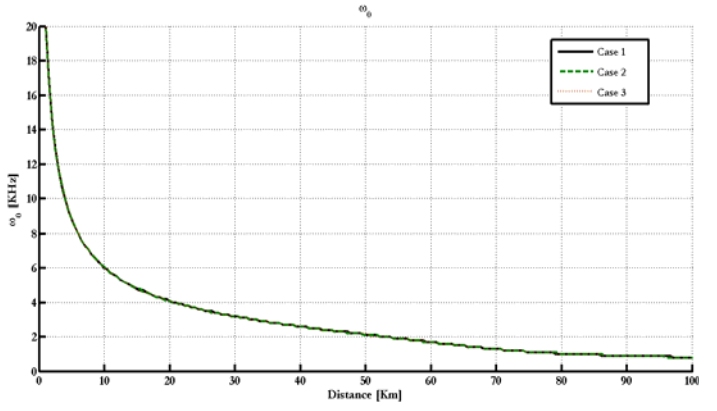

Fig. 4. Optimal frequency as a function of the range. There are not significant differences among the three studied cases.

Fig.s 5 to 8 show bandwith, capacity and power (in both heuristic and optimal definitions). Power is intended as the power required to achieve a 20 dB SNR gain. Similarly to the optimal frequency shown in Fig. 4, the bandwith is not influenced by the propagation conditions; this may appear surprising at first, since bandwidth does depend on the SNR. However, bandwidth depends on the relative differences of the SNR at adjacent frequencies; while the absolute SNR level is different from case to case, this is not so for the relative differences, hence the invariance of bandwidth with respect to environmental conditions. Differently from the bandwith, the reason why the capacity is apparently not affected by the propagation conditions in Figs. 7 and 8 is that here the source power compensates for SNR differences.

Finally, in Figs. 7 and 8, it can also be noted that at long ranges the environmental condition of case 2 (with both transmission ends within the thermocline region) is the one requiring the maximum power from the transmitter, while there are shorter ranges in which the most power consuming environmental conditions is the one of case 2 (transmitter and receiver on the opposite sides of the thermocline). In any case, the presence of the thermocline is detrimental to the system power consumption.

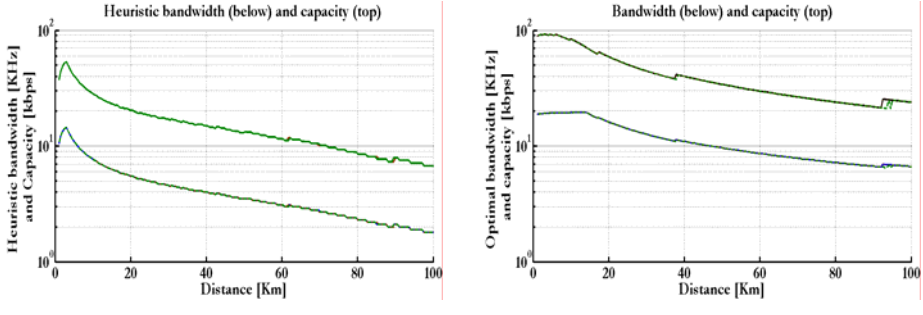

Fig. 5-6. The heuristic bandwith and capacity are shown on the left, while the optimal bandwith and capacity are on the right. There are not visible differences among the three studied cases.

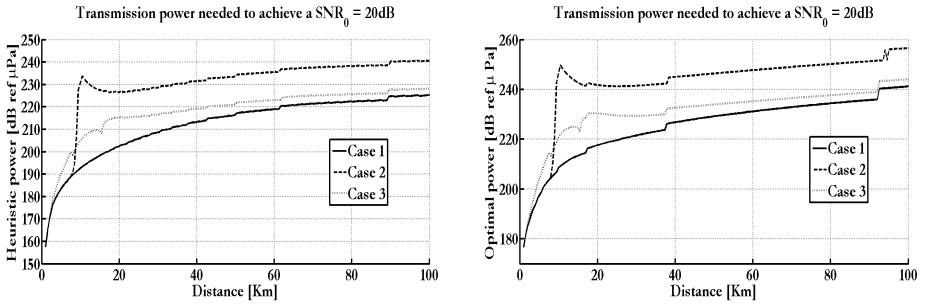

Fig. 7-8. On the left heuristic power and on the right optimal power required to achieve an SNR greater than 20 dB. Now differences among the three studied cases are evident.

3.2 Operational Scenario

The three cases considered for the operational scenario, in terms of relative position and sound speed profile in the water column, are reported in Fig. 9. In the simulations, frequencies from 20Hz to 50KHz have been considered, at 100Hz steps. Horizontal range varies between 100m and 6000m; 100 range slices have been considered.

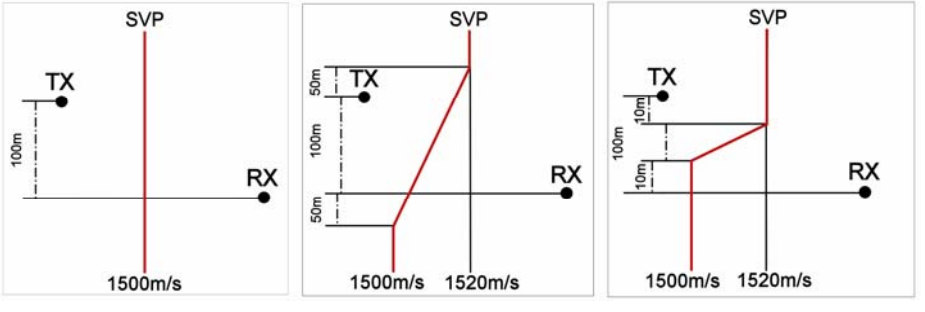

Fig. 9. The three cases considered, with different speed profiles as a function of depth, are shown from the left to the right

In Fig. 10 the SNR as a function of range is reported for the three cases; also in this scenario the SNR decreases when the direct path propagates through the thermocline.

In Fig. 11 the optimal propagation frequency is indicated for the three cases; while it is confirmed that also at higher frequencies the optimal frequency is not influenced by the propagation condition, here it is worth noting that the there is no optimal frequency above 38 KHz; the curve flattens at the 20 KHz value slightly above 1000m because 20 KHz is the inferior range considered in the scenario.

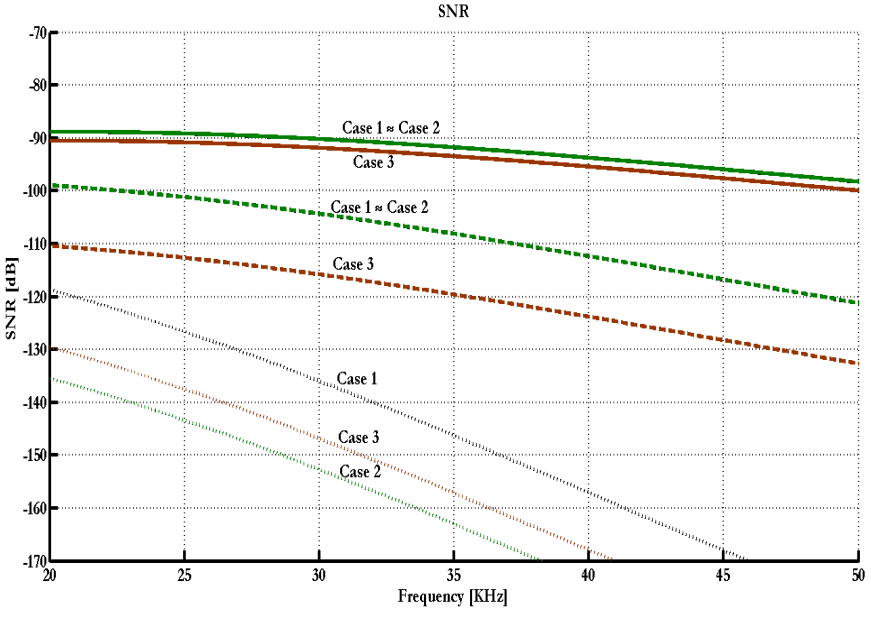

Fig. 10. SNR as a function of frequency. Solid lines refer to a range of 1 Km, dashed lines to range equal to 2 Km and dotted lines to 5 Km. For each of the three ranges, graphs corresponding to three cases are shown.

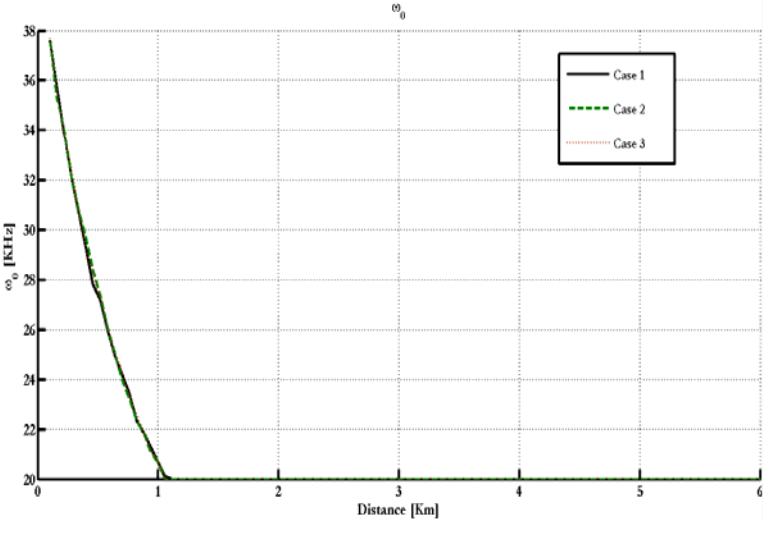

Fig. 11. Optimal frequency as a function of the range. There are not significant differences among the three studied cases.

Figs. 12 and 13, reports bandwidth and channel capacity (heuristic and optimal definition) while Figs. 14 and 15 report the required source power as a function of range to achieve a 20 dB SNR gain; here, in both cases, are more evident the nonlinear variations with range in the required power when propagation within the thermocline is considered.

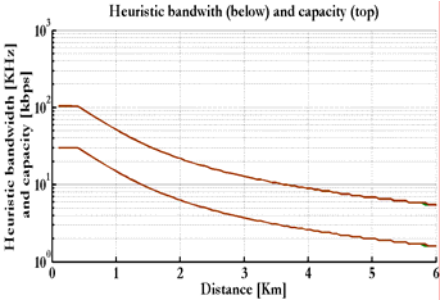

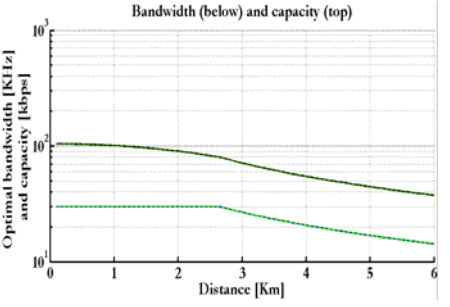

Fig. 12-13. On the left, heuristic bandwith and capacity as a function of the distance, while on the right the optimal bandwith and capacity are shown. There are not significant differences among the three studied cases.

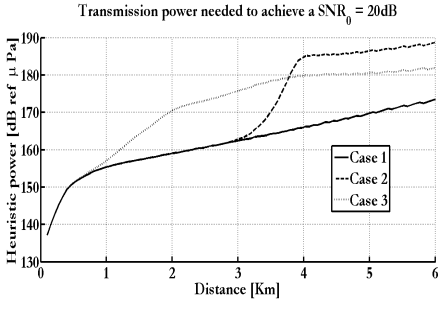

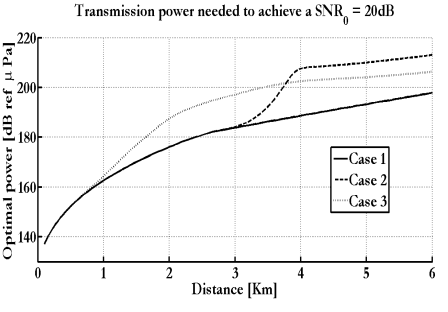

Fig. 14-15. On the left the heuristic power and on the right the optimal power required to achieve an SNR greater than 20 dB are shown. Now differences among the three studied cases are evident.

4 Discussion and Conclusions

In this work we have applied the theory developed in [1] to the computation of the underwater communication channel characteristics through the use of acoustic propagation simulators. In this way it is possible to consider the effective environmental conditions of the acoustic channel. This capability can be exploited in various ways: in the field, the on-line measurement of the sound speed profile in the water column (or equivalently the measurement of temperature and salinity) may be used to adapt on-line the characteristics of the communication system. At the design stage, sensitivity studies can be performed, similarly to what has been done in this contribution, analyzing particular environmental situations. In this paper such a sensitivity study

has been carried out considering the very frequent situation in which a thermocline region is present in the water column. While the main result may not come as a surprise (the best situation, from the point of view of communication performance, is when both transmitter and receiver are either above or below the thermocline), the sensitivity analysis shows how the transmission power, and hence the source level, is influenced in order to achieve a prescribed SNR. The same results can be used to determine, with a given source level, what is the maximum range at which transmitter and receiver can be positioned to guarantee a prescribed SNR.

As discussed in the paper, the numerical results obtained are subject to a series of assumptions that may not apply to any underwater communication system or environmental situation. In addition to the multi-path arrival contribution to the SNR, discussed in section 2.3, another notable effect not included in this study and that must be part of a thorough analysis of communication strategies for an AOSN is the Doppler effect due to relative transmitter-receiver motion. Our future work will develop on two directions: on one side, we will enhance the communication-oriented modeling of the acoustic channel; on a parallel line, we intend to exploit the results of sensitivity studies similar to the one reported here in order to devise collective motion strategies in AOSN that guarantee some quality of service requirements in the communication and networking.

Acknowledgments. This work has been partially supported by European Union, project UAN – Underwater Acoustic Networks, 7th Framework Programme, grant agreement no. 225669.

References

1. Stojanovic, M.: On the Relationship Between Capacity and Distance in an Underwater Acoustic Communication Channel. ACM SIGMOBILE Mobile Computing and Communications Review (MC2R) 11(4), 34–43 (2007)
2. Curtin, T., Bellingham, J., Catopovic, J., Webb, D.: Autonomous Oceanographic Sampling Networks. Oceanography 6(3), 86–94 (1993)
3. Anderson, B., Crowell, J.: Workhorse AUV – A cost-sensible new Autonomous Underwater Vehicle for Surveys/ Soundings, Search & Rescue, and Research. In: Proc. IEEE Oceans 2005 Conference (2005)
4. Alvarez, A., Caffaz, A., Caiti, A., Casalino, G., Gualdesi, L., Turetta, A., Viviani, R.: Fòlaga: A low-cost autonomous underwater vehicle combining glider and AUV capabilities. Ocean Engineering 36(1), 24–38 (2009)
5. Paley, D.A., Zhang, F., Leonard, N.E.: Cooperative Control for Ocean Sampling: The Glider Coordinated Control System. IEEE Trans. Control Systems Technology 16(4), 735–744 (2008)
6. Curtin, T.B., Bellingham, J.: Progress toward autonomous ocean sampling networks, Deep Sea Research – Part II. Topical studies in Oceanography (2008) (in press), doi:10.1016/j.dsr2.2008.09.005
7. Jensen, F., Kuperman, W., Porter, M., Schmidt, H.: Computational Ocean Acoustics. American Institute of Physics (AIP), New York (1995)

8. Chitre, M., Shahabodeen, S., Stojanovic, M.: Underwater Acoustic Communications and Networking: Recent Advances and Future Challenges. Marine Technology Society Journal 42(1), 103–116 (2008)
9. Ocean Acoustic Library, http://oalib.hlsresearch.com/
10. Caiti, A., Casalino, G., Lorenzi, E., Turetta, A., Viviani, R.: Distributed adaptive environmental sampling with AUVs: Cooperation and team coordination through minimum-spanning-tree graph searching algorithms. In: Proc. IFAC Conf. Navigation, Guidance and Control of Underwater Vehicles, Killakoe, Ireland (2008)
11. Ghabcheloo, R., Aguiar, A.P., Pascoal, A., Silvestre, C.: Coordinated Path-Following Control of Multiple Auvs in the Presence of Communication Failures and Time Delays. In: Proc. IFAC Conf. Manoeuvering and Control of Marine Crafts, Lisbon (2006)
12. Coates, R.: Underwater Acoustic Systems. Wiley, New York (1989)
13. Telatar, I.E.: Capacity of multi-antenna Gaussian channels. Eur. Trans. Telecom. 10, 585–595 (1999)